Effect of Film Morphology on the Energy Transfer to Emissive Green Defects in Dialkyl Polyfluorenes

Lynn J. Rozanski, Craig W. Cone, David P. Ostrowski, and David A. Vanden Bout*

Department of Chemistry and Biochemistry, Center for Nano and Molecular Science and Technology, and Texas Materials Institute, University of Texas at Austin, Austin, Texas 78712

Received March 12, 2007; Revised Manuscript Received April 19, 2007

ABSTRACT: The formation of a ketone defect at the 9-site along the backbone of dialkyl polyfluorenes has been shown to be directly involved in the degradation of the polymer's emission from blue to an undesirable green. Films of poly(9,9′-dihexylfluorene) (PFH) with and without ketone defects were annealed above their liquid crystalline phase transition in an inert argon atmosphere, and their emission spectra were collected in order to study the effect of morphology on the energy transfer to ketone defects. The annealing was performed in situ in the fluorometer, allowing for a direct comparison of the absolute changes in the emission spectra. Annealing of the films resulted in regions of highly aligned polymer chains as confirmed by atomic force microscopy. After annealing, the fluorescence spectra of pristine films (without ketone defects) exhibited no green emission, indicating the lack of thermal oxidation in the inert atmosphere. However, these films did show an increase in fluorescence quantum yield, revealing that high polymer order does not lead to interchain electronic species that quench the excited states. Annealing of partially photobleached PFH films revealed that an increase in the polymer chain order of a film containing a few defects resulted in an increase in green emission and decrease in blue without the creation of further defects. The increase in green emission combined with the decreased blue can only be the result of increased energy transfer from pristine chromophores to ketone sites, as the aligned polymer chains increase exciton diffusion. PFH films containing defects that were annealed beneath the LC temperature of the polymer did not result in any spectral changes, indicating that alignment of polymer chains was necessary for the increased energy transfer to the defect sites.

Introduction

Polyfluorenes (PFs) and their copolymers are one class of semiconducting conjugated polymers that show promise for use in various electronics such as light-emitting devices (LEDs),[1−5] photovoltaics,[6−8] and field effect transistors.[9,10] Polyfluorene in particular is one of few available blue-emitting conjugated polymers; its high quantum yield and thermal stability[11] make it quite promising as an active material in optoelectronic devices. Unfortunately, it has been observed that polyfluorene-based LEDs degrade with use, producing an overall decrease in emission intensity and undesirable red shift in wavelength toward a green emission.[12−15] While this low-energy emission band was initially believed to be from interchain species such as aggregates or excimers,[16−19] others have presented evidence that the emission was directly related to oxidative defects formed along the polymer backbone.[20−27,29−32] Synthetic fluorene/fluorenone copolymers with fluorescence emission that matched that of degraded films further supported the relation between these ketone defects and green emission.[25−27]

Yet there is still debate over the exact nature of this green emission; Sims et al. proposed a new theory that an excimer between ketone defects was required for green emission.[28] This new idea has ignited a fresh debate over the exact nature of the green peak, with recent papers testing the ketone excimer theory. Thorough examination of model fluorene/fluorenone oligomers and single molecule studies of similar copolymers refute the ketone excimer theory, demonstrating that a singular defect in the presence of pristine chromophores is enough to produce green emission.[29−32] However, other papers that have studied the photodegredation of PFO isolated between nanoparticles claim that the intermolecular interactions are necessary for green emission.[33] A recent electrochemical study has also found another green emission band that is distinct from that observed in the fluorene/fluorenone copolymer that is assigned to cross-linked fluorenes.[34] A clear understanding of the green emission is further complicated by the role of morphology and energy transfer and the quantification of the green emission. Most studies have not examined film morphology, making a direct comparison between the different studies difficult. Comparisons are also complicated because quantification of the green emission is often done by comparing the ratio of the emission peaked at 440 nm to that at 550 nm. Since the appearance of the green emission coincides with a decrease in the blue, this ratio can often be misleading; thus, a better means of quantifying green emission is to measure changes in both this ratio and the absolute intensity.

In previous papers a combination of polarization near-field optical scanning microscopy (NSOM) and atomic force microscopy (AFM) were used to infer the degree of polymer order between poly(dialkylfluorenes) of varying side-chain lengths.[17,35−37] The shorter side chain of poly(9,9′-dihexylfluorene) (PFH) displayed a higher degree of order after annealing to its liquid crystalline (LC) temperature than the longer side chain poly(9,9′-dioctylfluorene) (PFO) more commonly seen in the literature, so PFH has been the focus of these studies in order to show the greatest effect of intermolecular interaction with defect sites. In the previous measurements it appeared that increasing the chain order led to an increase in green emission that could be attributed to intermolecular interactions.[17,35−37] This was particularly the case in the PFH.[17] However, given the dramatic changes that were observed, it is possible that some of the annealing in inert atmospheres may have, in fact, not been completely free of oxygen or water vapor. It has been

---

* To whom correspondence should be addressed: e-mail davandenbout@mail.utexas.edu, Ph 1(512) 232-2824, Fax 1(512) 471-8696.

10.1021/ma0706069 CCC: $37.00

demonstrated that thermal annealing in the presence of oxygen led to ketone defects;[21] therefore, it is possible that the annealing led to changes in both film morphology and the number of ketone defects. If this was the case, what then is the role, if any, for film morphology? NSOM studies of pristine films not subjected to thermal treatment also showed a trend in which increased polymer order led to an increase in the green emission.[37] The effect of morphology cannot be discounted, as intensive research and modeling on conjugated polymers has shown the influence of film morphology on charge transport within films, where polymer chain orientation can increase charge transport.[39−44] Since ketone sites appear to behave as low-energy traps,[29−32] increased transport within the film will enhance their quenching effect. Whether increased ordered leads to longer exciton diffusion distances is an open question. Studies in PPV derivatives have shown that a reduction in energetic disorder improves exciton diffusion. However, there is a simultaneous reduction in excited-state lifetime.[45] In annealed MEH−PPV films this shortened lifetime has been attributed to interchain species that quench the excited state which forms as a result of increased ordering of the polymer chains.[46] The next effect is that while ordering of the polymer may lead to increased exciton diffusion, the ordering may also lead to an increase in interchain species that shortened lifetime and reduce the net diffusion distance.[45]

In this paper, the role of morphology on the green emission in PFH will be examined by comparison of the emission from films before and after annealing to their liquid crystalline phase transition temperature. In order to make a quantitative comparison, the annealing was performed in situ in the fluorometer so the samples could be probed under identical conditions and film orientations. This was due to the sensitivity of the instrument, where small differences in topography, film thickness, or angle relative to the incident excitation beam have a substantial effect on the fluorescence intensity. Great care was taken to control the inert atmosphere for annealing to prevent the oxidation of the films while heating. To study the role of morphology of films with ketone defects, films were photochemically bleached before annealing. The measurements all show that when carbonyl defects are initially present within the polymer film, an increase in the alignment of the polymer chains led to an increase in the green emission, the result of increased exciton diffusion to ketone sites, without the generation of further defects.

Results and Discussion

As has been shown previously in the literature, dialkyl polyfluorene films can be damaged photooxidatively as well as thermally in air to produce the expected[21,22] cyclic ketone carbonyl stretch in FTIR spectra around 1720 cm^{-1}. Fewer defects are formed thermally, producing a much weaker peak in the IR compared to photobleaching of the films (Supporting Information), and films annealed under nitrogen gas showed an increase in the green peak fluorescence without any evidence of carbonyl defects in the IR spectrum. This was indicative that a few defects, beneath the detection limit of the FTIR instrument, had a considerable effect on the fluorescence emission (Supporting Information). Since water vapor in the gas is a potential source of oxygen for ketone defects, dried argon gas was used to purge films to prevent the creation of ketone defects from air or water vapor. FTIR studies were performed on PFH films to ensure that defects were created within the films used for the morphology studies.

In order to directly compare the spectra before and after annealing, the heating of the sample was performed in situ in the fluorometer using a home-built heat cell designed to be purged with inert gas. In-situ data for a PFH thin film annealed under dried argon for 2 h are shown in Figure 1, exhibiting the structured blue emission characteristic of all poly(dialkylfluorenes), with maxima at 426, 450, and 480 nm. Direct comparison of the intensities of the emission before and after annealing requires a correction for the absorbance of the film at the excitation wavelength. Absorbance spectra taken before and after annealing (Supporting Information) showed a slight decrease in overall absorbance after annealing, likely due to the film forming ordered domains that have polarized absorption. Once the emission spectra were adjusted to account for the difference in the absorbance of the film at the excitation wavelength, the annealed emission was slightly higher than the pristine emission, indicating a slight increase in the quantum yield (Φ) upon annealing, as has been reported previously.[38] Figure 1 (inset) shows the pristine and annealed spectra normalized to have the intensity at 426 nm. The two spectra are indistinguishable, indicating no defects were created after prolonged annealing under the inert atmosphere. The increase in quantum yield also demonstrates that, unlike the PPV systems, an increase in polymer order does not lead to interchain species that quench the excited state. Rather, the annealing seems to remove some nonradiative decay paths, and the excited-state lifetime is enhanced.

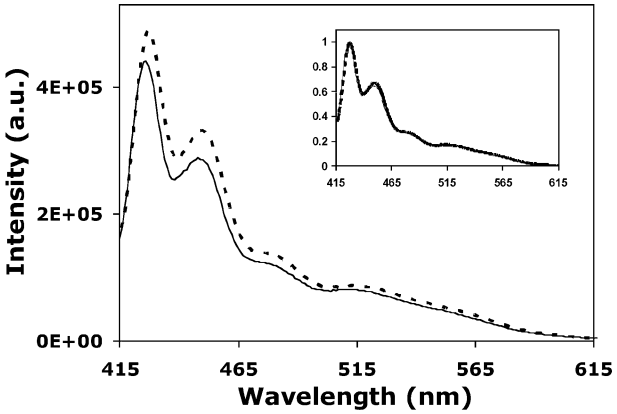

Figure 1. Pristine PFH emission (solid line) and after annealing under dried argon (dashed line). Both spectra normalized to the 426 nm blue peak (inset) showing no increase in green emission.

For comparison, the effect of defects on polyfluorene emission was also examined in situ for films annealed in air. The emission spectra, adjusted for the differences in the film's absorbance at the excitation wavelength, are shown in Figure 2. The creation of ketone defects after annealing is evident in the growth of a new, small broad peak at 525 nm, coupled with a pronounced decrease in intensity of the structured blue peaks. Annealing of the films in air changes both the order of the film and the number of defects (seen by the carbonyl peak in FTIR). Since these in-situ spectra show the absolute change in the film emission, it is apparent that the defects formed are highly effective at quenching blue emission, yet are not very emissive in of themselves, as only a minimal amount of green emission is produced after the creation of defects. Normalization of the two spectra to the first vibrational peak, shown in the inset of Figure 2, places emphasis on the green peak, showing its slightly greater intensity compared to the remainder of the blue peaks. Without a direct comparison of the spectra, this normalization to the first peak gives the impression that an extensive amount of green emission is produced, rather than an overall decrease in emission, seen by the in-situ spectra.

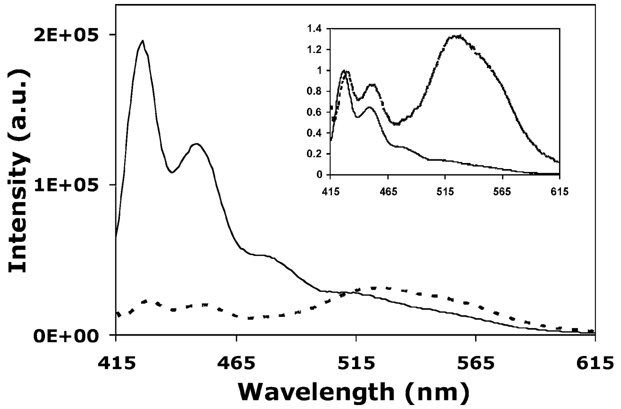

Figure 2. Pristine PFH film emission (solid line) and emission after film was annealed in air (dashed line). The spectra are normalized to the first blue peak, illustrating the increase in green emission (inset).

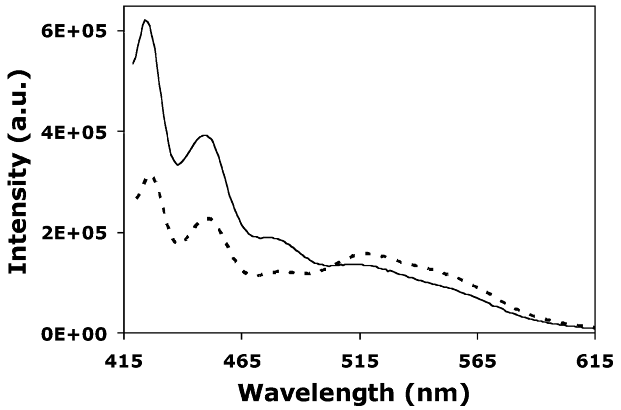

Figure 3. In-situ emission spectra of a partially photobleached PFH film prior to annealing (solid line) and after annealing (dashed line). The intensity of the blue emission decreased, and a slight growth in the green emission was also observed.

As there is no evidence of defects created when films are annealed under dry argon, it was possible to study the role of morphology on films already containing a small number of defects. To generate a few ketone defects, films were photobleached under a UV lamp for 40 min, enough to create a new broadened green peak at 520 nm in the spectrum, while not significantly quenching the blue peaks. Adjustment of the spectra for changes in absorbance did not change the final annealed emission; these spectra are shown in Figure 3. Prior to annealing, the spectrum retains much of the original blue intensity, with the green peak barely noticeable. Once annealed, the intensity of the blue emission decreased by half with a concomitant, but less intense, increase in the green emission. The absolute intensity changes of this in-situ data can be compared directly, and it is seen that the green emission has grown in intensity while the blue emission has decreased much more dramatically in comparison. No new defects were created as the annealing of the partially bleached film proceeded under dried argon, so this increase in the green peak must relate only to increased energy transport in the form of excitons to ketone defect sites as the polymer chains reorder into tightly packed domains. This increase cannot be explained by an increase in quantum yield, as that would have led to an increase of emission over the entire spectrum. The only explanation for the simultaneous decrease in blue emission and increase in green is that the high-energy blue excited state is funneled more efficiently to the lower energy defect sites after annealing, as no new defects have been created. Others have shown highly efficient intrachain energy transfer from pristine chromophores to defects on a single chain,[29−32] evidence that the ketone defect behaves as a low-energy trap. Although Dias et al.[32] examined the intermolecular energy transfer between polyfluorene and polyfluorene−fluorenone copolymers in solution, concluding that intermolecular energy transfer was inefficient, polymer chains in films are not isolated from neighboring chains as they are in solution, and increase in intermolecular energy transfer is seen when chains are well ordered and packed together.[47−49] The increase in green emission is likely not from newly formed excimer species in the annealed film; studies on similar rigid-rod PPE polymers have shown that the ordered polymer chains minimized the unfavorable close contacts required for excimers.[50]

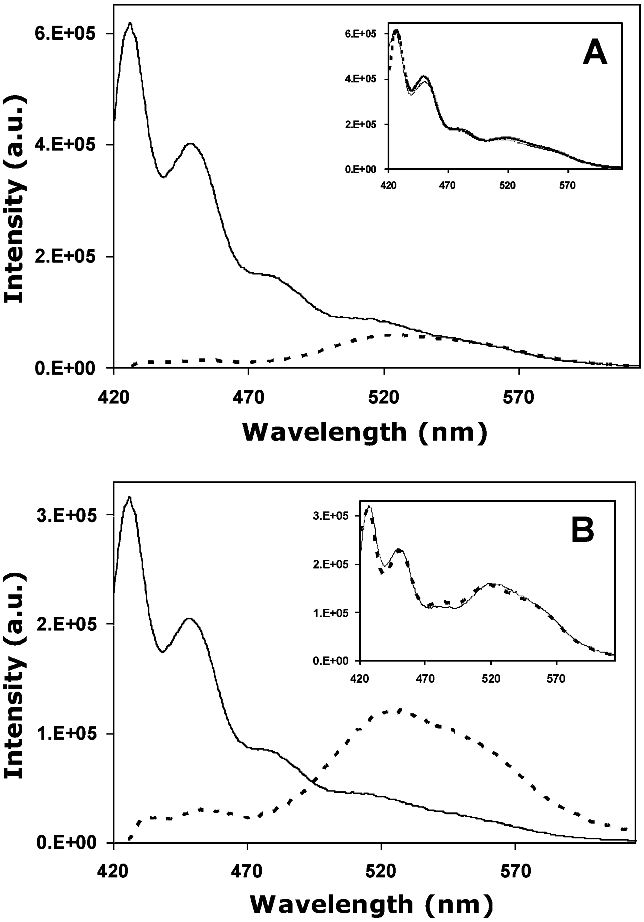

Figure 4. Model spectra for the partially bleached PFH film prior to annealing (A) and after annealing (B). For both, the generated blue spectrum (solid line) and green spectrum (dashed line) are combined (inset, dashed line) and overlaid with the actual emission spectrum (inset, solid line), with nearly identical overlay.

The degree of order within these films was examined by anisotropy measurements, which measure the degree of polarization, taken for all of the films (Supporting Information). Pristine films have an anisotropy of roughly 0.04 due to energy transfer among the disordered polymer segments that almost entirely washes out any polarization. Annealed PFH films have an increased degree of order, with anisotropy values of 0.14 for films annealed in air or under dried argon. The green emission in the partially bleached film annealed under dried argon has the largest film anisotropy (0.2). The large anisotropy value remains constant over the green emission, implying that the green emission is polarized in the same direction as the absorbance. This also indicates that energy transfer to the defects occurs predominately within ordered domains where the polymers have the same orientation. The anisotropies for the argon-

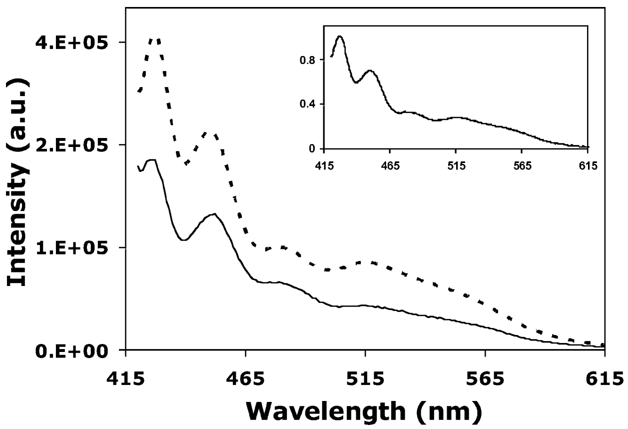

Figure 5. Partially bleached PFH film emission (solid line) and emission after heating to 150 °C for 2 h (dashed line). Both spectra normalized to the initial blue peak, showing an identical overlay.

annealed films contain a large peak on the blue edge of the spectrum that results from emission from the highest energy chromophores. These sites can only be populated by direct excitation, rather than through energy transfer, so they exhibit the highest degree of polarization.

Model spectra were created using singular value decomposition (SVD)[52] to quantitatively compare the spectra before and after annealing. The SVD was performed on the basis set of all of the spectra acquired. The SVD results indicated that the entire data set could be well represented by two basis spectra. A blue emission spectrum and green emission spectrum were created from this basis set, with one basis spectrum as essentially the blue spectrum and the green spectrum generated by adding a sufficient amount of the first basis spectrum to the second so that it had a positive value for all wavelengths. These two spectra were then used to fit all the acquired data simply by varying their relative amplitudes. Figure 4 shows the fit with the blue and green spectra for a PFH film bleached for 40 min under a UV lamp prior to annealing (A) and after annealing (B). The generated full spectrum, created through the addition of the two spectra, is shown overlaid with the experimental data in the inset of both graphs of Figure 4; the excellent fit allows for quantification of the blue and green emission. Prior to annealing under dried argon, the ratio of the blue emission to the green emission in Figure 5 is 5.12; this ratio drops to 1.31 after annealing. Since both the blue and green emission change by different amounts, a comparison of the fits of just the blue or green emission reveals that the area of the blue intensity decreased 48.8% after annealing, whereas the area of the green intensity increased 103%. From these numbers alone it appears that the green emission has grown dramatically to have a higher intensity than the blue emission; however, taking into account that the blue emission was 5 times as large as the green emission initially, the decrease in blue was considerably larger than the increase in green. The overall emission intensity decreased by 24.4% after annealing.

The increase in green emission has been attributed to an increase in energy transfer that results from the increased order of polymer chains, and to show that the aligned polymer chains were the source of increased green emission, a partially photobleached film was annealed at a temperature below the liquid crystal (LC) temperature of 250 °C for PFH. Heating the films at 150 °C for the same amount of time as the LC temperature annealed films provides heating of the film without ordering the chains into a liquid-crystalline phase. The emission spectra for the low-temperature annealed partially bleached PFH films, adjusted for their differences in absorption at the excitation wavelength, are shown in Figure 5. Similar to PFH annealed at its LC temperature, the emission spectra increase slightly in intensity after annealing under dried argon, showing a small increase in quantum yield. However, the inset in Figure 5 shows that the overlay of the annealed and the pristine emission spectra are completely indistinguishable; therefore, the increase in quantum yield did not lead to a change in the ratio of the blue to green emission.

Unlike the PFH film annealed at the LC temperature, the film heated at the lower temperature does not show any birefringence under cross-polarized illumination in a microscope, indicating a lack of micron-sized ordered domains in the film. Atomic force microscopy (AFM) images allow a comparison of the nanoscale ordering of the films. Figure 6 shows the AFM images of a film annealed at 150 °C and a film annealed at the liquid crystalline phase transition temperature. The topography of the lower-temperature heated film is very similar to that of the pristine film (Supporting Information), with both the pristine and the lower-temperature annealed films having a rough, disordered topography. This is in stark contrast to the topography of the film annealed at the LC temperature, which exhibits bundles of aligned ribbonlike structures that extend over many microns. Near-field scanning optical microscopy studies have demonstrated that these ribbonlike features are composed of aligned polymer chains.[33] Therefore, it is apparent that the increase in the green emission in the LC annealed and partially bleached film resulted from an increase in polymer order, allowing for more efficient energy transfer to the defect sites.[39,44] Without this alignment the only change is the slight increase in quantum yield with no increase in green emission.

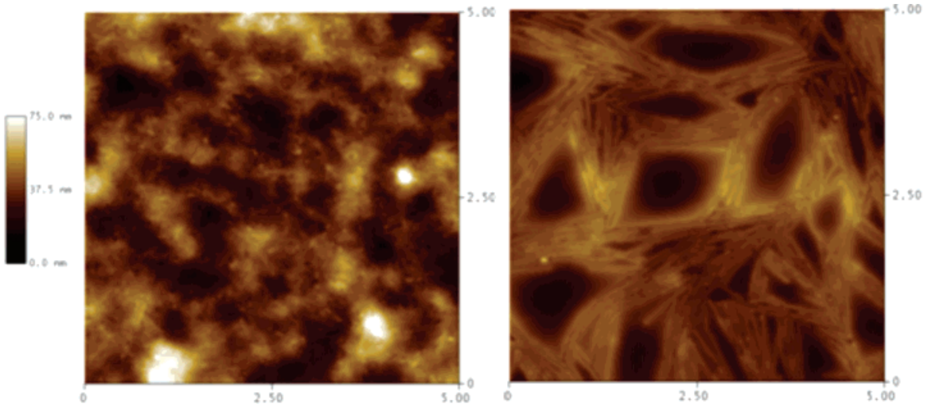

Figure 6. 5 × 5 μm AFM scans of PFH films annealed at 150 °C (left) for 2 h and 250 °C (right) for 2 h. The film annealed at 250 °C has its polymer chains reordering into long ribbonlike structures.

Conclusions

In-situ annealing of PFH films allowed for direct comparison of the absolute changes in emission spectra, and these changes were quantified using SVD basis spectra. Films annealed under dried argon showed no evidence of ketone defect formation; thus, it was possible to monitor the effect of increased film order on emission of a film already containing defects. An increase in green emission was seen in annealed films containing defects, evidence that increased polymer order led to increased diffusion of excitons from pristine chains to trapping defect sites. Quantification of the amount of blue and green emission supported this evidence, showing that energy from the blue emission was transferred more efficiently to the defect sites, producing more green emission. The increase in polymer chain order was definitively found to be the source of the increase in green emission and decrease in blue emission for films annealed to the LC temperature; thus, the reordering of polymer chains into tightly packed domains is required for the increased exciton diffusion to the few defect sites in the film. These results should be generic for other conjugated polymer systems in that increase order should lead to more efficient energy transfer. The caveat being that in some systems such as PPV derivatives increased order can also shorten the excited-state lifetime.[45,46] The results have important implications for polymer photovoltaics, as initial steps for generating charges within a polymer photovoltaic requires efficient exciton transport to heterojunctions.[53] The morphologies in these polymer solar cells are often limited as the exciton diffusion length is roughly 10 nm or less.[54] Thus, the use of aligned polymer chains can increase the exciton diffusion distances if interchain species can be minimized, allowing for more efficient movement of excitations to the charge separation heterojunctions.

Experimental Section

Poly(9,9-dihexylfluorene) from the Dow Chemical Co. was used without further preparation. Two types of films were made: 100 nm thin films for fluorescence measurements were spin-cast from 1% (w/w) solutions in chloroform onto cleaned glass or quartz substrates, and $\sim$1 μm thick films were drop-cast onto aluminum-coated silicon wafer for FTIR measurements. FTIR spectra were taken on a Thermo Mattson Infinity Gold FTIR with a Pike Technologies Veemax II variable angle grazing accessory at 60° incident angle; thick films were treated in an identical manner as the thin films used for in-situ measurements. In-situ fluorescence measurements were taken in a SPEX DM3000 fluorometer in front-face mode using a homemade holder with gas-purging capability and a thermocouple-regulated heat source. Thin films spin-cast on quarts substrates were sealed within the holder so that the film could be purged with dried argon; the excitation light went through the quartz substrate to excite the polymer film, minimizing surface roughness effects. With the exception of films annealed in air, all films were purged with dried argon for 1 h prior to heating to ensure thorough removal of oxygen and continued to be purged after annealing until they returned to room temperature. All annealed films were heated for 2 h, within ±1 °C of the temperature mentioned. Absorbance spectra were collected on a Cary 5000 UV−vis NIR spectrometer before and after annealing and underwent baseline correction. Topography measurements were taken on a Digital Instruments Multimode AFM in tapping mode.

Acknowledgment. This work was supported by the Robert A. Welch Foundation (F-1377). Thanks to the Center for Nano and Molecular Science and Technology for support and to the SPRING program of the AFOSR for their financial contribution.

Supporting Information Available: Absorbance spectra, anisotropy measurements, and AFM scans. This material is available free of charge via the Internet at http://pubs.acs.org.

References and Notes

(1) Friend, R. H.; Gymer, R. W.; Holmes, A. B.; Burroughes, J. H.; Marks, R. N.; Taliani, C.; Bradley, D. D. C.; Dos Santos, D. A.; Bredas, J. L.; Logdlund, M. L.; Salaneck, W. R. *Nature (London)* **1999**, *397*, 121.
(2) Nakazawa, Y. K.; Carter, S. A.; Nothofer, H.-G.; Scherf, U.; Lee, V. Y.; Miller, R. D.; Scott, J. C. *Appl. Phys. Lett.* **2002**, *80*, 3832.
(3) Grice, A. W.; Bradley, D. D. C.; Bernius, M. T.; Inbasekaran, M.; Wu, W. W.; Woo, E. P. *Appl. Phys. Lett.* **1998**, *73*, 629.
(4) Bernius, M. T.; Inbasekaran, M.; O'Brian, J.; Wu, W. *Adv. Mater.* **2000**, *12*, 1737.
(5) Leger, J. M.; Carter, S. A.; Kuhstaller, B.; Nothofer, H. G.; Scherf, U.; Tillman, H.; Horhold, H. H. *Phys. Rev. B* **2003**, *5*, 4209.
(6) Arias, A. C.; MacKenzie, J. D.; Stevenson, R.; Halls, J. J. M.; Inbasekaran, M.; Woo, E. P.; Richards, D.; Friend, R. H. *Macromolecules* **2001**, *34*, 6005.
(7) McNeill, C. R.; Frohne, H.; Holdsworth, J. L.; Dastoor, P. C. *Nano Lett.* **2004**, *4*, 2503.
(8) Kietzke, T.; Neher, D.; Kumke, M.; Montenegro, R. *Macromolecules* **2004**, *37*, 4882.
(9) Chua, L.; Zaumseil, J.; Chang, J.; Ou, E. C.-W.; Ho, P. K.−H.; Sirringhaus, H.; Friend, R. H. *Nature (London)* **2004**, *434*, 194.
(10) Sirringhaus, H.; Wilson, R. J.; Friend, R. H.; Inbasekaran, M.; Wu, W.; Woo, E. P.; Grell, M.; Bradley, D. D. C. *Appl. Phys. Lett.* **2000**, *77*, 406.
(11) Millard, I. S. *Synth. Met.* **2000**, *111*−*112*, 119.
(12) Bliznyuk, V. N.; Carter, S. A.; Scott, J. C.; Klärner, G.; Miller, R. D.; Miller, D. C. *Macromolecules* **1999**, *32*, 361.
(13) Weinfurtner, K. H.; Fujikawa, H.; Tokito, S.; Taga, Y. *Appl. Phys. Lett.* **2000**, *76*, 2502.
(14) Lee, J. I.; Klaerner, G.; Miller, R. D. *Synth. Met.* **1999**, *101*, 126.
(15) Pei, Q. B.; Yang, Y. *J. Am. Chem. Soc.* **1996**, *118*, 7416.
(16) Lemmer, U.; Heun, S.; Mahrt, R. F.; Scherf, U.; Hopmeier, M.; Siegner, U.; Göbel, E. O.; Müllen, K.; Bässler, H. *Chem. Phys. Lett.* **1995**, 373.
(17) Teetsov, J.; Vanden Bout, D. A. *Langmuir* **2002**, *18*, 897.
(18) Grell, M.; Bradley, D. D. C.; Ungar, G.; Hill, J.; Whitehead, K. S. *Macromolecules* **1999**, *32*, 5810.
(19) Cimrová, V.; Scherf, U.; Neher, D. *Appl. Phys. Lett.* **1996**, *69*, 608.
(20) List, E. J. W.; Guentner, R.; de Freitas, P. S.; Scherf, U. *Adv. Mater.* **2002**, *14*, 374.
(21) Gong, X.; Iyer, P. K.; Moses, D.; Bazan, G. C.; Heeger, A. J.; Xiao, S. S. *Adv. Funct. Mater* **2003**, *13*, 325.
(22) Hintschich, S. I.; Rothe, C.; Sinha, S.; Monkman, A. P.; de Freitas, P. S.; Scherf, U. *J. Chem. Phys.* **2003**, *119*, 12017.
(23) Lupton, J. M.; Craig, M. R.; Meijer, E. W. *Appl. Phys. Lett.* **2002**, *80*, 4489.
(24) Zojer, E.; Pogantsch, A.; Hennebicq, H.; Beljonne, D.; Bredas, J. L.; de Freitas, P. S.; Scherf, U.; List, E. J. W. *J. Chem. Phys.* **2002**, *117*, 6794.
(25) Gong, X.; Moses, D.; Heeger, A. J.; Xiao, S. *Synth. Met.* **2004**, *141*, 17.
(26) Dias, F. B.; Maiti, M.; Hintschich, S. I.; Monkman, A. P. *J. Chem. Phys.* **2005**, *122*, 054904.
(27) Romaner, L.; Pogantsch, A.; de Freitas, P. S.; Scherf, U.; Gaal, M.; Zojer, E.; List, E. J. W. *Adv. Funct. Mater.* **2003**, *13*, 597.
(28) Sims, M.; Bradley, D. D. C.; Ariu, M.; Koeberg, M.; Asimakis, A.; Grell, M.; Lidzey, D. G. *Adv. Funct. Mater.* **2004**, *14*, 765.
(29) Pogantsch, A.; Zaami, N.; Slugovc, C. *Chem. Phys.* **2006**, *322*, 399.
(30) Becker, K.; Lupton, J. M.; Feldmann, J.; Nehls, B. S.; Galbrecht, F.; Gao, D.; Scherf, U. *Adv. Funct. Mater.* **2006**, *16*, 364.
(31) Chi, C.; Im, C.; Enkelmann, V.; Ziegler, A.; Lieser, G.; Wegner, G. *Chem.*−*Eur. J.* **2005**, *11*, 6833.
(32) Dias, F. B.; Knaapila, M.; Monkman, A. P.; Burrows, H. D. *Macromolecules* **2006**, *39*, 1598.
(33) Aharon, E.; Albo, A.; Kalina, M.; Frey, G. L. *Adv. Funct. Mater.* **2006**, *16*, 980.
(34) Montilla, F.; Mallavia, R. *Adv. Funct. Mater.* **2007**, *17*, 71.
(35) Teetsov, J.; Vanden Bout, D. A. *J. Am. Chem. Soc.* **2001**, *123*, 3605.
(36) Teetsov, J.; Fox, M. A. *J. Mater. Chem* **1999**, *9*, 2117.
(37) Teetsov, J.; Vanden Bout, D. A. *J. Phys. Chem. B* **2000**, *104*, 9387.
(38) Asada, K.; Kobayashi, T.; Naito, H. *Jpn. J. Appl. Phys.* **2006**, *45*, L247.
(39) Hennebicq, E.; Pourtois, G.; Scholes, G. D.; Herz, L. M.; Russel, D. M.; Silva, C.; Setayesh, S.; Grimsdale, A. C.; Müllen, K.; Bredas, J.-L.; Beljonne, D. *J. Am. Chem. Soc.* **2005**, *127*, 4744.

(40) Sreearunothiaj, P.; Morteani, A. C.; Avilov, I.; Cornil, J.; Beljonne, D.; Friend, R. H.; Phillips, R. T.; Silva, C.; Herz, L. M. *Phys. Rev. Lett.* **2006**, *96*, 117403.
(41) Nguyen, T.-Q.; Yee, R. Y.; Schwartz, B. J. *J. Photochem. Photobiol. A* **2001**, *144*, 21.
(42) Nguyen, T.-Q.; Schwartz, B. J. *J. Chem. Phys.* **2002**, *116*, 8198.
(43) Schwartz, B. J. *Annu. Rev. Phys. Chem.* **2003**, *54*, 141.
(44) Wong, K. F.; Bagchi, B.; Rossky, P. J. *J. Phys. Chem. A* **2004**, *108*, 5752.
(45) Markov, D. E.; Tanase, C.; Blom, P. W. M.; Wildeman, J. *Phys. Rev. B* **2005**, *72*, 045217−1.
(46) Nguyen, T. Q.; Martini, I. B.; Liu, J.; Schwartz, B. J. *J. Phys. Chem. B* **2000**, *104*, 237.
(47) Prins, P.; Grozema, F. C.; Nehls, B. S.; Farrell, T.; Scherf, U.; Siebbeles, L. D. A. *Phys. Rev. B: Condens. Matter Mater. Phys.* **2006**, *74*, 113203/1.
(48) Chou, H.; Lin, K.; Fan, Y.; Wang, D. *J. Polym. Sci., Part B: Polym. Phys.* **2005**, *43*, 1705.
(49) Lee, T.; Park, O. O. *Adv. Mater.* **2000**, *12*, 801.
(50) Bunz, U. H. F.; Imhof, J. M.; Bly, R. K.; Bangcuyo, C. G.; Rozanski, L.; Vanden Bout, D. A. *Macromolecules* **2005**, *38*, 5892.
(51) Zhao, W.; Cao, T.; White, J. M. *Adv. Funct. Mater.* **2004**, *14*, 783.
(52) Henry, R.; Hofrichter, J. *Methods Enzymol.* **1992**, *210*, 129.
(53) Snaith, H. J.; Friend, R. H. *Thin Solid Films* **2004**, *451*, 567.
(54) Ramsdale, C. M.; Bache, I. C.; MacKenzie, J. D.; Thomas, D. S.; Arias, A. C.; Donald, A. M.; Friend, R. H.; Greenham, N. C. *Physica E* **2002**, *14*, 268.

MA0706069